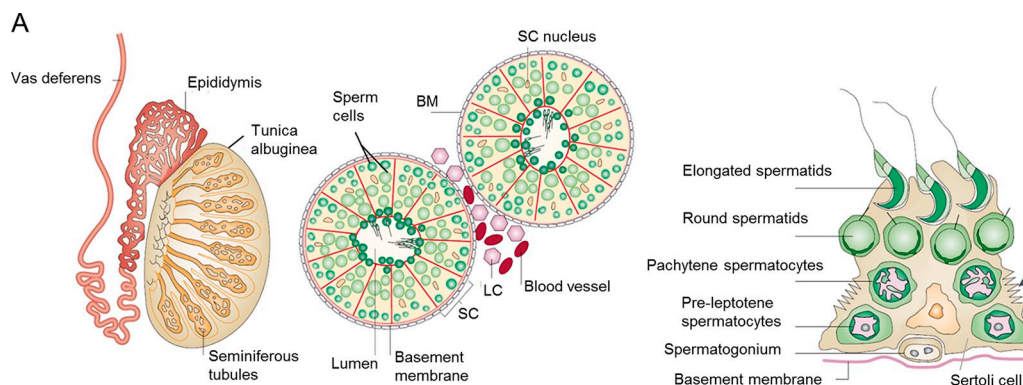


Holembowski et al., <http://www.jcb.org/cgi/content/full/jcb.201306066/DC1>**B** TAp73KO mice are largely infertile

	WT/Het	TAp73KO - 1 st mating trial	TAp73KO - 2 nd mating trial
Age of males	7 - 8 weeks	7 - 8 weeks	10 - 14 weeks
Mating number	4	19	12
Ability to produce offspring	4	8	4
Percentage	100	42	33

C No difference in testis size and weight of adult p73KO and WT mice

	young mice (P20)		adult mice (P42-70)	
	WT	p73KO	WT	p73KO
size in mm	5.6 +/-0.5 x 4 +/-0.3	5.1 +/-0.7 x 3.8 +/-0.6	7.8 +/-0.7 x 5 +/-0.5	7.9 +/-0.7 x 5.2 +/-0.5
weight in mg	47 +/- 12.3	31.4 +/- 3.6 *	130 +/- 23.7	122 +/- 34.5

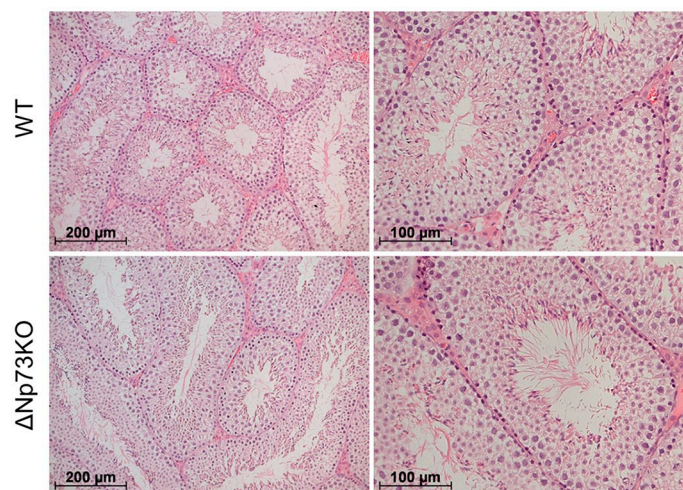
D P49

Figure S1. $\Delta Np73$ mice show normal testicular morphology. This figure is related to Fig. 1. p73KO mice are infertile and TAp73KO mice are largely infertile. (A) Anatomical (left) and histological (middle and right) organization of testis. (Middle) A schematic cross section of seminiferous tubules. (Right) Germ cells develop in nursing pouches of a Sertoli cell, which houses up to 50 germ cells at different stages. Sertoli cells are anchored at the BM and stretch up into the lumen of the seminiferous tubule. SC, Sertoli cell; BM, basement membrane; LC, Leydig cell in extratubular stroma. Reprinted by permission from Macmillan Publishers Ltd: *Nature Reviews Genetics* (Cooke and Saunders, 2002). (B) TAp73KO mice are largely infertile. Heterozygous females were mated with either WT/Het or TAp73KO males for 4 wk each. The absolute number of conducted matings and the ability to produce offspring is indicated. About 40% of young TAp73KO males were still able to produce some healthy offspring, but this declined with age. Independent of genotype, litter sizes were between 4 and 10 offspring. (C) Quantitation of testis size and weight of young (P20, $n = 5-6$) and adult (P42-P70, $n = 7-13$) mice per genotype. Adult p73KO testes are similar in size and weight. Developing p73KO testes (P20) are slightly smaller and significantly lighter. Their lower testicular weight can be explained by the smaller-size young KO mice being outcompeted for food by their WT littermates in mixed litters. Upon separation, KO pups grow to mice of regular weight and size. *, $P < 0.05$ (*t* test). (D) Sections of testes comparing $\Delta Np73$ KO and WT mice at stage P49. No germ cell loss can be observed in isoform-specific young KO mice. They show normal testicular morphology. H&E staining is shown.

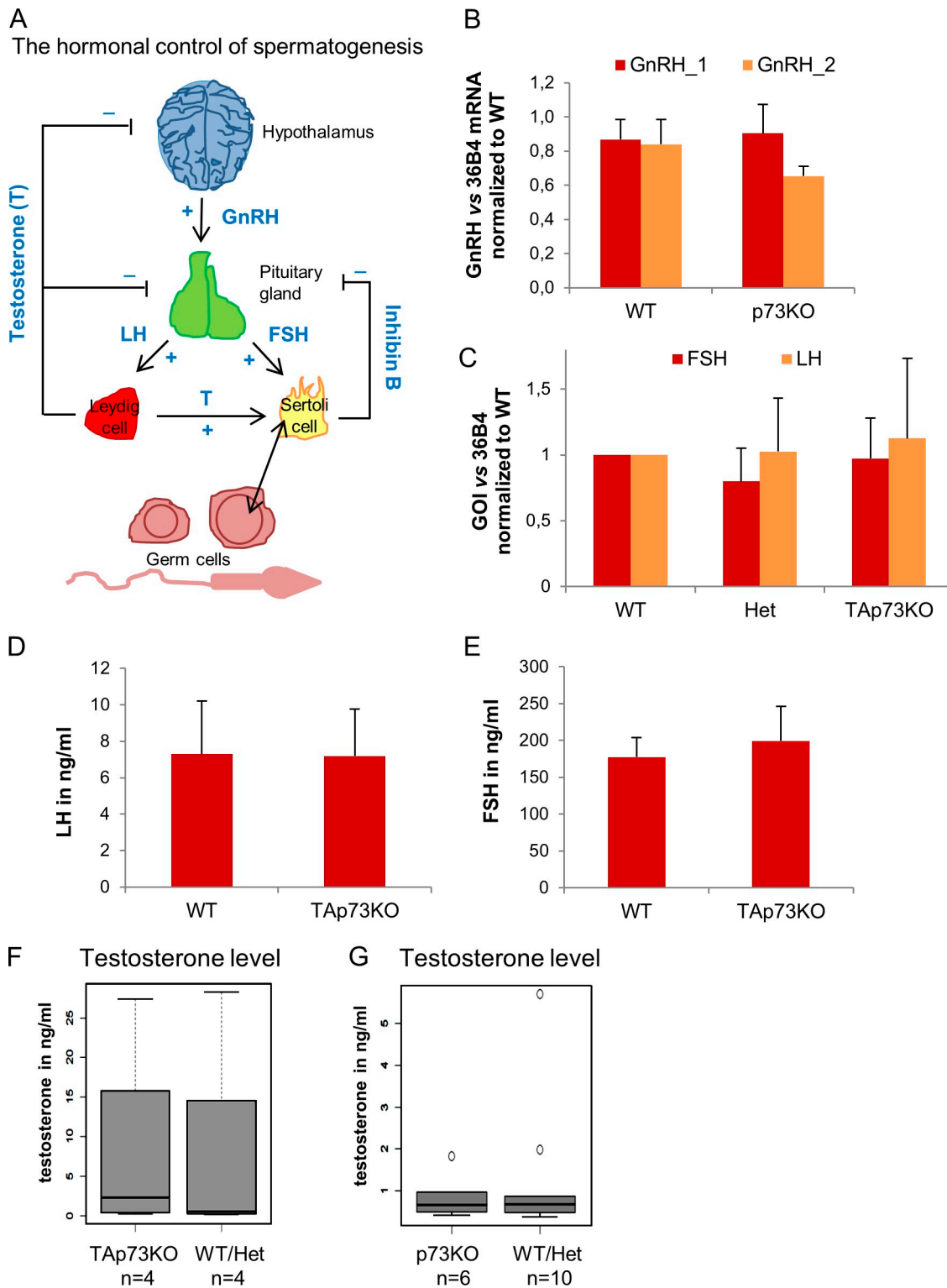


Figure S2. **The hormonal hypothalamic–pituitary–testicular axis is normal in p73KO and TAp73KO mice.** This figure is related to Fig. 2. (A) Hormonal control of spermatogenesis occurs via the hypothalamic–pituitary–testicular axis. (B–G) Expression levels of all hormones are normal in p73KO and TAp73KO mice. (B and C) Quantitation of GnRH-1 and GnRH-2 isoforms (mRNA isolated from brain, $n = 3$ mice per genotype) and of FSH and LH (mRNA isolated from the pituitary gland, $n = 5$ – 10 mice per genotype) of adult KO and WT mice by qRT-PCR. KO levels are comparable to WT levels. (D and E) Quantitation of serum LH (D) and FSH (E) hormone levels from an ELISA immunoassay. $n = 4$ – 5 adult mice per genotype. KO levels of both hormones are comparable to WT levels. (F and G) Adult TAp73KO (F) and total p73KO (G) mice have normal serum testosterone levels. Measurement by ELISA immunoassays on the indicated number of mice is shown. (B–G) For all quantitations, t tests were applied. No significant differences were found. Error bars indicate mean \pm SD.

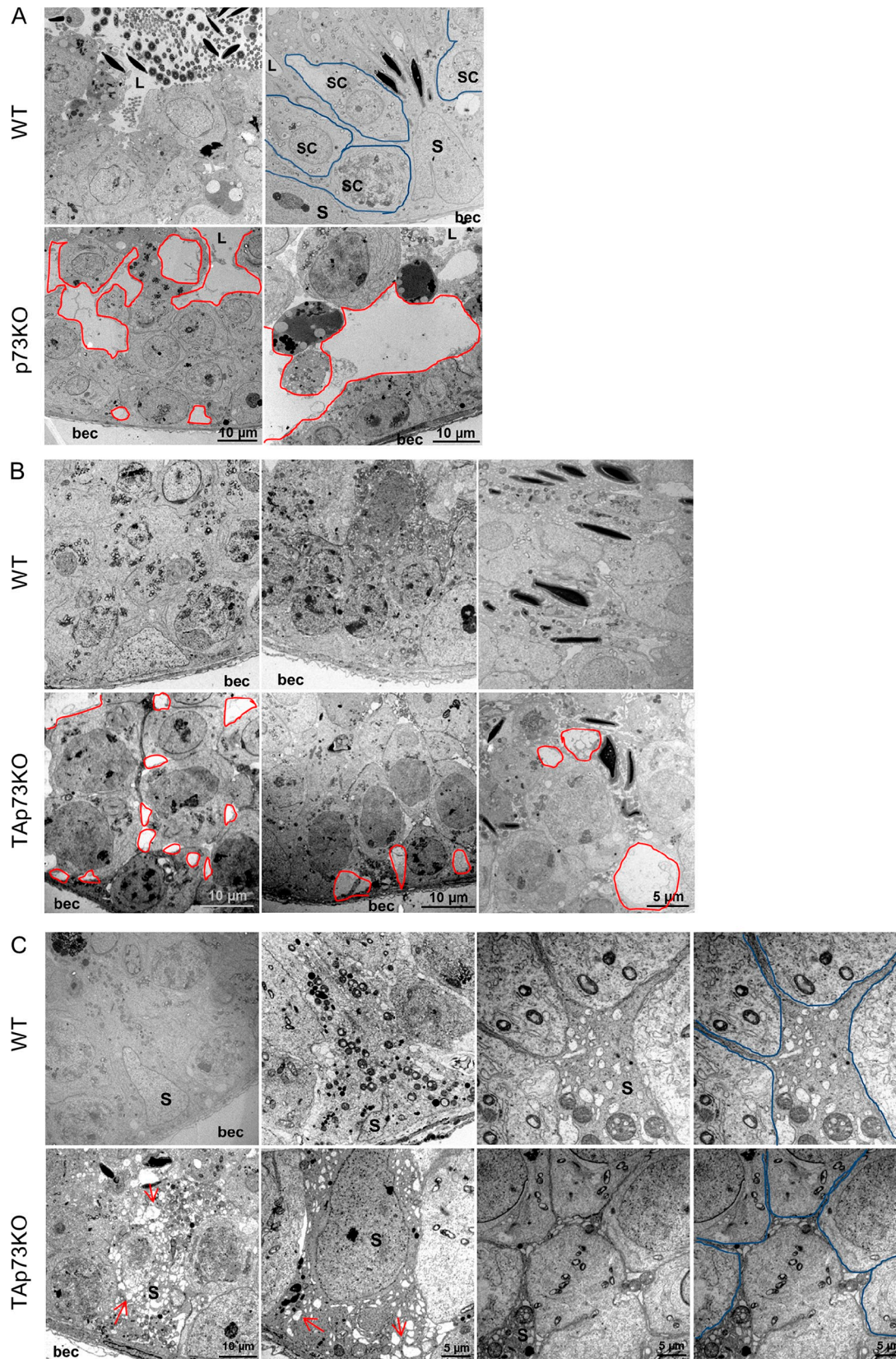


Figure S3. **The structure of the seminiferous epithelium and Sertoli cell morphology are severely impaired in p73KO and TAp73KO mice.** This figure is related to Fig. 4. (A–C) Electron microscopy of ultrathin sections from seminiferous tubules of adult testis of p73KO (A) and TAp73KO (B and C) mice compared with WT littermates. In KO testis, late stage developing immature germ cells (SC) fail to properly attach to each other and to Sertoli cells, hence cells lose contact with the surrounding epithelium (A). Frequently, large lacunar gaps (shown in red) are present between germ cells and between germ and Sertoli cells in KO epithelium (A and B), whereas WT testes display a tightly packed adhesive seminiferous epithelium with only mature spermatozoa (the dark elongated structures) detaching from the apical layer into the lumen (L; A and B). Moreover, in contrast to WT, KO Sertoli cells (S) reveal degenerate morphology, characterized not only by cell–cell gaps, but also by greatly increased cytoplasmic vacuolization (arrows), thinning (blue outline), and loss (not depicted; see Fig. 4 C) of cytoplasmic arms that form the nursing pouches (C). bec, basal extracellular. Representative images from 2–5 mice per genotype are shown.

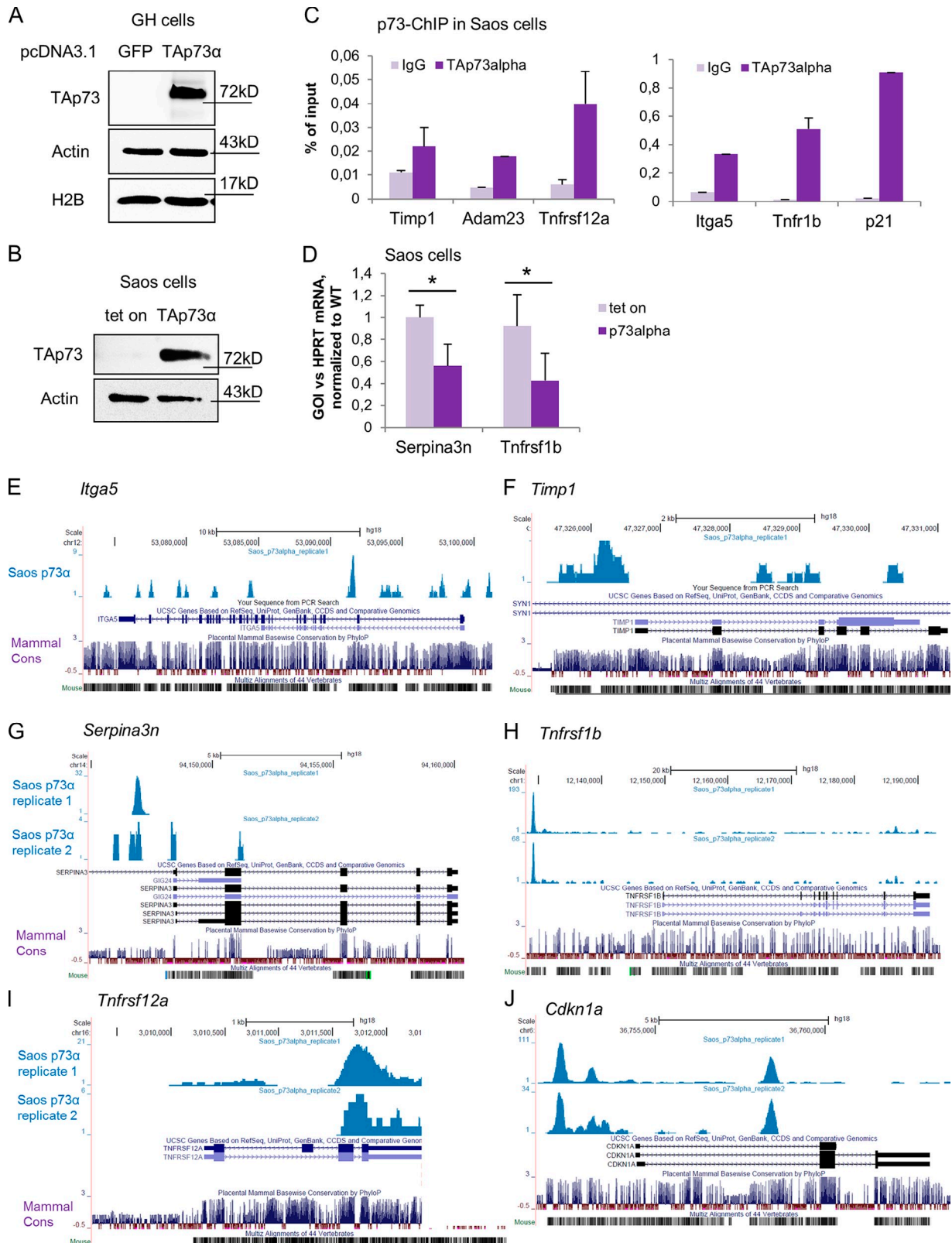


Figure S4. **TAp73 directly binds to gene loci of adhesion and migration-associated genes and regulates their transcription.** This figure is related to Fig. 5. (A) Control immunoblot for Fig. 5 (F and G) showing transient overexpression of TAp73α in the chromatin fraction of GH testicular carcinoma cells. The TAp73-specific antibody ab14430 was used to detect p73 in immunoblots and in ChIP analyses. H2B serves as a positive control for the nuclear fraction. (B) Control immunoblot for C and D showing inducible overexpression of TAp73α in Saos-2 cells. Tet-on-only plasmid was transfected as a negative control. The TAp73-specific antibody ab14430 was used to detect p73 in immunoblots and ChIP analyses. (C) Binding of TAp73α to the promoters of the indicated adhesion-related genes was validated with targeted ChIP assays from chromatin of Saos-2 cells inducibly overexpressing TAp73α. Binding to the gene of interest over IgG control is shown. Results are depicted as percentage of input. (D) Transcriptional suppression of *Serpina3n* and *Tnfrsf1b* in Saos-2 cells overexpressing TAp73α compared with “tet-on” control. A qRT-PCR assay is shown. $n = 3$ independent samples, mean \pm SD (error bars). *, $P < 0.05$ (*t* test). (E–J) ChIP sequencing analysis of Saos-2 cells inducibly overexpressing human TAp73α. TAp73α binding to the loci of the indicated adhesion-associated human genes is illustrated with the UCSC genome browser. Displayed are two biological replicas for *Serpina3n* (G), *Tnfrsf1b* (H), and *Tnfrsf12a* (I). For *Itga5* (E) and *Timp1* (F), only one replica is shown. *Cdkn1a* (P21; J) serves as a positive control. The conservation of the TAp73 binding site between human and mouse on each gene is shown using the vertebrate MultiZ Alignment and the mammal conservation track from the UCSC genome browser.

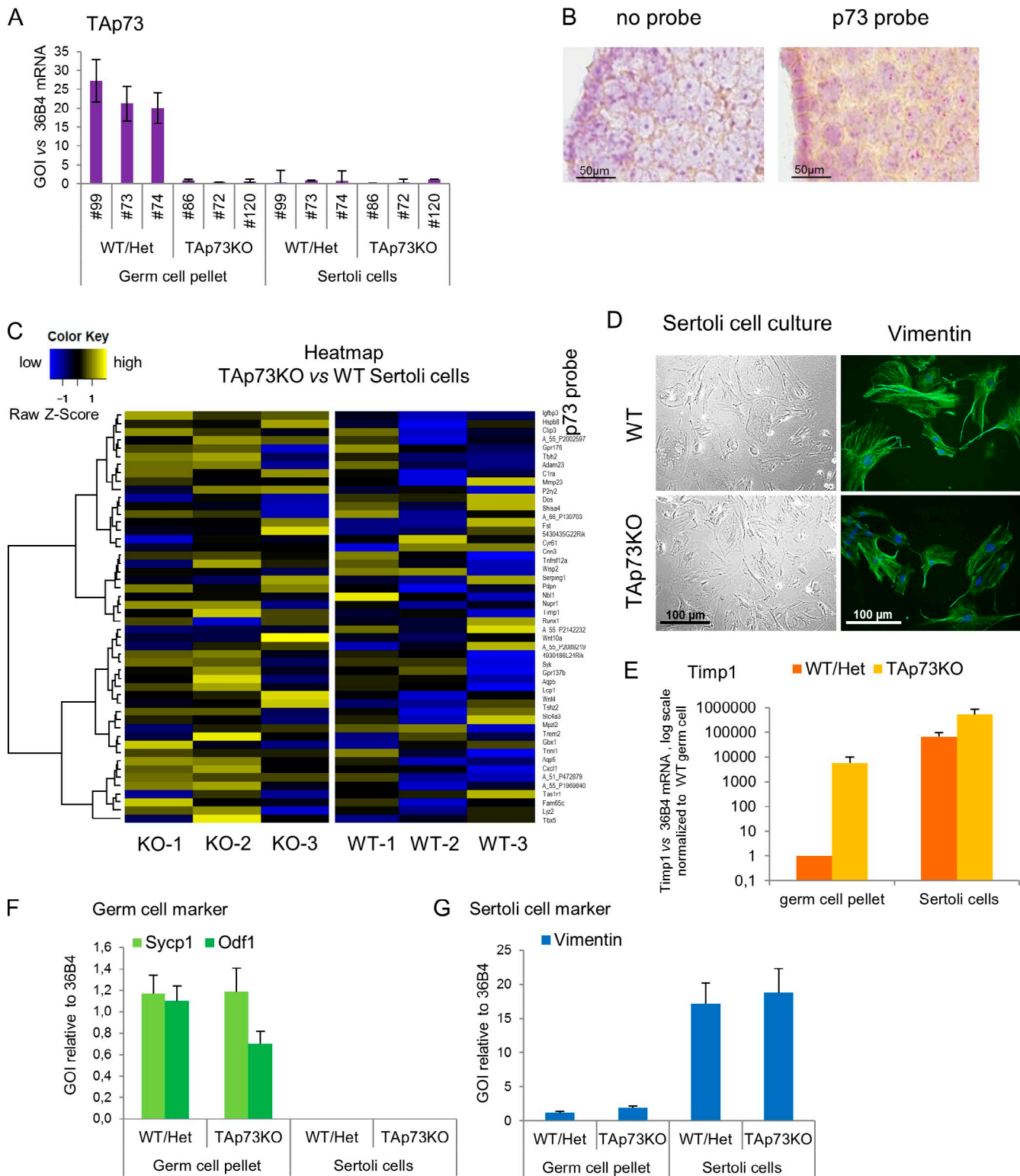


Figure S5. **TAp73 does not modulate the transcriptional program of Sertoli cells.** This figure is related to Fig. 6. (A) TAp73 is exclusively expressed in WT germ cells, whereas WT Sertoli cells (P0) have undetectable levels like KO controls. qRT-PCR, $n = 3$ mice per fraction. (B) RNA in-situ hybridization for TAp73 in WT seminiferous epithelium. Signal for TAp73 mRNA (pink dots with irregular sizes) shows TAp73 expression in germ cells. "Control probe" was exposed to nonspecific cDNA only. Both images are also shown in Fig. 6 B. (C) Sertoli cell-specific microarray analysis of shortly cultured Sertoli cells (P0) isolated from adult TAp73KO and WT littermates. $n = 3$ mice/genotype. The heat map shows the top 50 genes that were differentially regulated in KO germ cells (see Fig. 6 C). No change in expression pattern of these genes was found for Sertoli KO cells. (D) Primary in vitro culture of murine Sertoli cells isolated from adult TAp73KO and WT testes. Cultured Sertoli cells show comparable morphology. Immunostaining with the Sertoli marker Vimentin is shown. (E) Expression of Timp1 mRNA isolated from germ cell pellet or cultured Sertoli cells of TAp73KO and WT/Het testes. qRT-PCR is shown. Timp1 is strongly up-regulated in KO germ cells, but expression is not changed in Sertoli cells ($n = 3-5$ mice each). (F and G) Control qRT-PCR of cell fractions. Expression of Sycp1 (meiotic germ cell marker) and Odf1 (spermiogenic germ cell marker) in the germ cell pellet only (F) and expression of Vimentin (Sertoli cell marker) in cultured Sertoli cells only (G) show the purity of the two fractions. Results represent mean \pm SD.

Table S1. Adhesion- and migration-associated genes are deregulated in whole TAp73KO testis

Candidate rank	Gene	Description	NCBI gene ID	Log fold change (KO to WT)	P-value (KO to WT)
3	<i>Timp1</i>	Timp1	21857	3.82	1.44×10^{-7}
16	<i>Serpina3n</i>	Serine (or cysteine) peptidase inhibitor, clade A, member 3N	20716	3.01	1.73×10^{-6}
27	<i>Tnfrsf12a</i>	Tumor necrosis factor receptor superfamily, member 12a	27279	2.44	7.02×10^{-6}
37	<i>Itgax</i>	Integrin alpha X	16411	1.86	1.01×10^{-5}
67	<i>Serpinb6b</i>	Serine (or cysteine) peptidase inhibitor, clade B, member 6b	20708	1.45	1.40×10^{-4}
90	<i>Serping1</i>	Serine (or cysteine) peptidase inhibitor, clade G, member 1	12258	1.25	5.80×10^{-6}
93	<i>Adam23</i>	A disintegrin and metallopeptidase domain 23	23792	1.24	1.89×10^{-6}
98	<i>Itga5</i>	Integrin alpha 5 (fibronectin receptor alpha)	16402	1.23	5.32×10^{-6}
108	<i>Serping1</i> ^a	Serine (or cysteine) peptidase inhibitor, clade G, member 1	12258	1.19	3.31×10^{-6}

A significant number of differentially regulated genes are associated with adhesion and migration (26 of 159, 16.4%), and nearly all of these are up-regulated with TAp73KO testis. Many of the differentially regulated proteins have a proteinase inhibitory function, some possess peptidase activity, and others are part of intercellular junctions and cell-matrix adhesion. The table lists, for each gene, its rank within the 159 genes, its name, and its NCBI gene ID. Induction is depicted as log₂ since the threshold is set at twofold. A positive number indicates up-regulation in TAp73KO mice versus WT mice. The fold induction can be calculated by 2^x. Up-regulation of all depicted genes could be validated by qPCR.

^aTwo different microarray spots, representing this gene, were analyzed.

Table S2. Deregulated adhesion- and migration-associated genes in KO testis and germ cells

Gene	Description	NCBI gene ID	Log fold change (KO to WT)	P-value (KO to WT)
<i>Timp1</i> ^a	Tissue inhibitor of metalloproteinase 1	21857	3.82	1.44×10^{-7}
<i>Gpnmb</i> ^a	Glycoprotein (transmembrane) nmb	93695	3.77	1.45×10^{-3}
<i>Mpzl2</i> ^a	Myelin protein zero-like 2	14012	3.33	1.30×10^{-5}
<i>Wnt4</i> ^a	Wingless-related MMTV integration site 4	22417	3.18	3.79×10^{-7}
<i>Serpina3n</i>	Serine (or cysteine) peptidase inhibitor, clade A, member 3N	20716	3.01	1.73×10^{-6}
<i>Tnfrsf12a</i> ^a	Tumor necrosis factor receptor superfamily, member 12a	27279	2.44	7.02×10^{-6}
<i>Spp1</i> ^a	Secreted phosphoprotein 1	20750	1.99	2.53×10^{-3}
<i>Itgax</i>	Integrin alpha X	16411	1.86	1.01×10^{-5}
<i>Sykb</i> ^a	Spleen tyrosine kinase	20963	1.57	1.69×10^{-5}
<i>Aplp1</i>	Amyloid beta (A4) precursor-like protein 1	11803	1.55	3.51×10^{-5}
<i>Serpinb6b</i>	Serine (or cysteine) peptidase inhibitor, clade B, member 6b	20708	1.45	1.40×10^{-4}
<i>Ddr1</i>	Discoidin domain receptor family, member 1	12305	1.41	6.00×10^{-6}
<i>Clec7a</i>	C-type lectin domain family 7, member a	56644	1.41	8.71×10^{-6}
<i>P2ry2</i> ^a	Purinergic receptor P2Y, G-protein coupled 2	18442	1.39	6.73×10^{-6}
<i>Col11a1</i>	Collagen, type XI, alpha 1	12814	1.39	5.29×10^{-3}
<i>Serping1</i> ^a	Serine (or cysteine) peptidase inhibitor, clade G, member 1	12258	1.25	5.80×10^{-6}
<i>Adam23</i> ^a	A disintegrin and metallopeptidase domain 23	23792	1.24	1.89×10^{-6}
<i>Ccr5</i>	Chemokine (C-C motif) receptor 5	12774	1.23	2.34×10^{-5}
<i>Itga5</i>	Integrin alpha 5 (fibronectin receptor alpha)	16402	1.23	5.32×10^{-6}
<i>Tnfrsf1b</i>	Tumor necrosis factor receptor superfamily, member 1b	21938	1.18	2.48×10^{-4}
<i>Dpt</i>	Dermatopontin	56429	1.13	1.64×10^{-3}
<i>Eda</i>	Ectodysplasin-A	13607	1.07	3.92×10^{-5}
<i>Spink8</i>	Serpin, Kazal type 8	78709	1.05	3.00×10^{-4}
<i>Pdpr</i> ^a	Podoplanin	14726	1.05	1.19×10^{-4}
<i>Mmp23</i> ^a	Matrix metallopeptidase 23	26561	1.04	9.40×10^{-4}
<i>Cldn10</i>	Claudin 10	58187	-1.11	1.19×10^{-3}

Microarray analysis of TAp73KO testis compared to WT revealed that 16.4% (26 of 159) of all deregulated genes in KO are associated with adhesion or migration. The table lists the gene name and the respective NCBI gene ID. Induction is given as log₂ since the threshold is set at twofold. A positive number indicates up-regulation in TAp73KO mice versus WT mice, while a negative number indicates down-regulation. The fold induction is calculated by 2^x.

^aGenes that also come up in the germ cell-specific microarray.

Table S3. Murine primers used for qRT-PCR in this study

Primer name	Sequence (5'→3')
qPCR-Adam23 fwd	TGTCCTTGGGGGCACAGCT
qPCR-Adam23 rev	TCCGGCAGCATGGCTGAAAACA
qPCR-Clec7a fwd	CTTCACCTTGGAGGCCATT
qPCR-Clec7a rev	AGGGAGCCACCTTCTCATCT
qPCR-FSHβ fwd	CAGTAGAGAAGGAAGAGTGCCG
qPCR-FSHβ rev	CGGTCTCGTATACCAGCTCC
qPCR-GnRH fwd1	GGGTGGCCCTGGGGAAA
qPCR-GnRH rev1	CTGAGGGGTGAACGGGGCCAG
qPCR-GnRH fwd2	CCCCGTTACCCCTCAGGGAT
qPCR-GnRH rev2	CCACCTGGGCCAGTGCACTAC
qPCR-Gpnmb fwd	CTGGGAGATGATGCAAGCCT
qPCR-Gpnmb rev	CTTTCCGGTGACTGAGGAGA
qPCR-Ilgax fwd	GGCAGCTGTCTCCAAGTTGCTCA
qPCR-Ilgax rev	TGGTGCTCCAACCACCACCCA
qPCR-Igta5 fwd	CGGTGCCCAAGGGGAACCTC
qPCR-Igta5 rev	AGCAGGGGTGCCCTACCAG
qPCR-LHβ fwd	GCCGGCCTGTCAACGCAACT
qPCR-LHβ rev	TGGGGTCTACACCCGGTGGG
qPCR-Mmp23 fwd	CCCACAGCTACAGTTGGAA
qPCR-Mmp23 rev	ACAAAATCCGGTCCAGGCA
qPCR-Mpz12 fwd	GGACGATCCGGCTCAGCGTT
qPCR-Mpz12 rev	GCACTGTCCGCCATCGCTT
qPCR-Odf1 fwd	TGCTGCTGCGACCTGCATCC
qPCR-Odf1 rev	GCTCGAGCAAGACGAGGCCA
qPCR-P2ry2 fwd	GGGAGAGCCATTACGTGAC
qPCR-P2ry2 rev	CTGGGACTGAGGCAGGAAAC
qPCR-Pdpn fwd	GAGGAACCTGTCCACCTCAGC
qPCR-Pdpn rev	TGGTAACAAGACGCCAACT
qPCR-Serpina3n fwd	CAGCAGCCTCGTCAGGCCAA
qPCR-Serpina3n rev	GCCTCTCTTGCCCGGTAG
qPCR-Serpin6b fwd	TGCTGACAGCCTGAACCTGGGG
qPCR-Serpin6b rev	GCCAGGGCTGAGGAGACGCT
qPCR-Serping1 fwd	GGAGCCGCTTGCTCAGTGCTC
qPCR-Serping1 rev	GCTCTTGGTGCTGTCTCCAGCC
qPCR-Spp1 fwd	GCTGTGCTCTGAAGAAAAGG
qPCR-Spp1 rev	GGACATCGACTGTAGGGACG
qPCR-Sycp1 fwd	CAAAAGCCCTTACACTGTTCTGTC
qPCR-Sycp1 rev	CTCCTTCTGATAGTGACAACTGCC
qPCR-Syk fwd	CCCATGAGAAGATGCCCTGG
qPCR-Syk rev	GAGAGCTTCCCGTCTTGTC
qPCR-Timp1 fwd	CACCAGAGCAGATACCATGATGGC
qPCR-Timp1 rev	TATCTGCGGCATTTCCACAGC
qPCR-Tnfrsf12a fwd	TTCTTGCCCTCGGACCGGCA
qPCR-Tnfrsf12a rev	TTGTGAGGTCGGCGCTCCA
qPCR-Vimentin fwd	AGGAGCTGCAGGCCAGATTCA
qPCR-Vimentin rev	GCAGGGCATCGTTGTTCCGGT
qPCR-Wnt4 fwd	GTACCTGGCCAAGCTGTCATCGG
qPCR-Wnt4 rev	GTATACAAAGGCCGCTCCCGG
qPCR-36B4 fwd	GCAGATCGGGTACCCAACCTGTTG
qPCR-36B4 rev	CAGCAGCCGCAAATGCAGATG

fwd, forward; rev, reverse.

Table S4. Murine p73 primers used for PCR genotyping and qRT-PCR in this study

Primer name	Sequence (5'→3')
PCR p73common fwd	GGCCATGCCTGTCTACAAGAA (binds to Exon 5)
PCR p73WT rev	CCTTCTACACGGATGAGGTG (binds to Exon 6)
PCR p73KO rev	GAAAGCGAAGGAGCAAAGCTG (binds to Neo cassette)
PCR TAp73common fwd	CTGGCCCTCTCAGCTTGTGCCACTTC (binds to Intron 1-2)
PCR TAp73WT rev	CTGGTCCAGGAGTGAGACTGAGGC (binds to Intron 1-2)
PCR TAp73KO rev	GTGGGGTGGGATTAGATAAATGCCTG (binds to Neo cassette)
qPCR-p73pan fwd	GGCCATGCCTGTCTACAAGAA
qPCR-p73pan rev	GATGGTGGTAAATTCGTGTTCC
qPCR-TAp73 fwd	GAGCACCTGTGGAGTTCTCTAGAG
qPCR-TAp73 rev	GGTATTGGAAGGGATGACAGGGC
qPCR-ΔNp73 fwd	GTGTGCAGACCCCCACGAGC
qPCR-ΔNp73 rev	GGTATTGGAAGGGATGACAGGGC

fwd, forward; rev, reverse.

Table S5. Rat primers used for qRT-PCR in this study

Primer name	Sequence (5'→3')
qPCR-Acr fwd	CGACCTGTGTAACCTCCACCC
qPCR-Acr rev	CGTGATCCCCACGATCACAA
qPCR-Sycp1 fwd	TCGGCTGTGAAACCTCAGAC
qPCR-Sycp1 rev	CAACCTGTTCAAGCATGGGC
qPCR-36B4 fwd	ATCGTCTTTAAACCCCGCGT
qPCR-36B4 rev	GCATCATGGTGTCTTGGCC

fwd, forward; rev, reverse.

Table S6. Human primers used for ChIP and qRT-PCR analysis in this study

Primer name	Sequence (5'→3')
ChIP Adam23 fwd	TGTAATTTCCCTGTGCCAGA
ChIP Adam23 rev	CCACCCTGAAGGACTGAGAA
ChIP Cldn10 fwd	GATCTCCATCCTGCACATTC
ChIP Cldn10 rev	TTGCTATAAAGTCGGCAAG
ChIP Clec7a fwd	CTCGTGGCTTGATAGAATC
ChIP Clec7a rev	GATCTAGGAGCTGGTAGGG
ChIP EDA fwd	ACTTGTTTCATGGCCCAGAG
ChIP EDA rev	CACACAACCTCAGCATTGACC
ChIP Gpnmb fwd	AACACACAGGTTCCCAGGAG
ChIP Gpnmb rev	TCATGGGCTCTGACTCACC
ChIP Itga5 fwd	GAGATTCAAGCCAGGTCAGC
ChIP Itga5 rev	AGACCAGTGGCGAGTTCTA
ChIP p21 fwd	GCAGATGTGGCATGTGTCC
ChIP p21 rev	AGTGACTGCACGACCTTGG
ChIP P2ry2 fwd	AGAGCCCTGTTAGGGTTAGG
ChIP P2ry2 rev	TCAGCAGTTGGGTAATCTGG
ChIP Serpina3n fwd	CAGAGATTCAAGCCAGGTCAG
ChIP Serpina3n rev	CCTGGGCAACACAGAGAGAC
ChIP Serpinb6b fwd	AACTGTTGACCCGATGAAC
ChIP Serpinb6b rev	CATGTGTGATGGCAGGACAG
ChIP Timp1 fwd	GCCACCTGAGTTCAGTCTC
ChIP Timp1 rev	AGGCACGGAGTGGTTAAGTG
ChIP Tnfrsf1b fwd	GGCCTCTTCTGTTCTGTGG
ChIP Tnfrsf1b rev	CGACATGCCCAGAGTTACAG
ChIP Tnfrsf12a fwd	ATGCCGCAGGAGAGAGAAG
ChIP Tnfrsf12a rev	GGGCTGCAAGATAAGAGGTG
ChIP Wnt4 fwd	CTTTCCCAGTGTACCCACAG
ChIP Wnt4 rev	CAACACAGCAAGCATCTGAC
qPCR-HPRT fwd	ATGCTGAGGATTTGAAAAGG
qPCR-HPRT rev	TCATCACATCTCGAGCAAGAC
qPCR-Itga5 fwd	GCTCAGAGGGAGAGGAGCCTG
qPCR-Itga5 rev	AGTAACCCTGTCCTGCTGCC
qPCR-Serpina3n fwd	ATGGGAGATGCCCTTTGACC
qPCR-Serpina3n rev	TCATGGGCACCATTACCCAC
qPCR-Serping1 fwd	GATGCTATTCGTTGAACCCATC
qPCR-Serping1 rev	CAGTAGTGGGCTGGGTAGGA
qPCR-Timp1 fwd	CCTTCTGCAATTCGACCTC
qPCR-Timp1 rev	CTGGTTGACTTCTGGTGTCCTC
qPCR-Tnfrsf12a fwd	CAGGCTCCACCATGGCTC
qPCR-Tnfrsf12a rev	GGTCGGCCCTGCAAGAC
qPCR-Tnfrsf1b fwd	TGTGACAGCCTTGGGTCTAC
qPCR-Tnfrsf1b rev	TTATCGGCAGGCAAGTGAGG

fwd, forward; rev, reverse.

Table S7. Description of constructs used for lentiviral assays

Construct name	Backbone/vector	Promoter	GenBank accession number	Clone ID	Source
TIMP1	pLOC	CMV	DQ894301	PLOHS_100008761	Thermo Fisher Scientific
ITGA5	pLOC	CMV	EU176722	PLOHS_100011505	Thermo Fisher Scientific
TNFRSF12A	pLOC	CMV	DQ896216	PLOHS_100005598	Thermo Fisher Scientific
SERPINA3	pLX304	CMV	BC034554	ccsbBRoad304_05752	Thermo Fisher Scientific
SERPING1	pLOC	CMV	DQ891799	PLOHS_100004429	Thermo Fisher Scientific
GFP	pHR'SIN-cPPT-SEW	SFFV	DQ896216		A gift from A.G. von Laer, Georg-Speyer-Haus, Frankfurt, Germany
VSV-G	pMD2.G	CMV	12259	Addgene ID 12259	A gift from A.G. Grez, Georg-Speyer-Haus
8.91	pCMVΔ8.91	CMV		Plasmid factory Bielefeld	A gift from A.G. Grez

CMV, cytomegalovirus.

Reference

Cooke, H.J., and P.T. Saunders. 2002. Mouse models of male infertility. *Nat. Rev. Genet.* 3:790–801. <http://dx.doi.org/10.1038/nrg911>